Thermal transpiration through single walled carbon nanotubes and graphene channels

Joe Francis Thekkethala and Sarith P. Sathian

Citation: The Journal of Chemical Physics **139**, 174712 (2013); doi: 10.1063/1.4828705
View online: http://dx.doi.org/10.1063/1.4828705
View Table of Contents: http://scitation.aip.org/content/aip/journal/jcp/139/17?ver=pdfcov
Published by the AIP Publishing

Thermal transpiration through single walled carbon nanotubes and graphene channels

Joe Francis Thekkethala and Sarith P. Sathian[a)]
Computational Nanotechnology Laboratory, School of Nano Science and Technology, National Institute of Technology Calicut, Kozhikode, Kerala - 673601, India

(Received 11 July 2013; accepted 14 October 2013; published online 7 November 2013)

Thermal transpiration through carbon nanotubes (CNTs) and graphene channels is studied using molecular dynamics (MD) simulations. The system consists of two reservoirs connected by a CNT. It is observed that a flow is developed inside the CNT from the low temperature reservoir to the high temperature reservoir when the two reservoirs are maintained at different temperatures. The influence of channel size and temperature gradient on the mean velocity is analysed by varying the CNT diameter and the temperature of one of the reservoirs. Larger flow rate is observed in the smaller diameter CNTs showing an increase in the mean velocity with increase in the temperature gradient. For the flow developed inside the CNTs, slip boundaries occur and the slip length is calculated using the velocity profile. We examine the effect of fluid-wall interaction strength (ε_{fw}), diffusivity (D), and viscosity of the fluid (μ) on the temperature induced fluid transport through the CNTs. Similar investigations are also carried out by replacing the CNT with a graphene channel. Results show that the mean velocity of the fluid atoms in the graphene channel is lower than that through the CNTs. This can be attributed to the higher degree of confinement observed in the CNTs. © *2013 AIP Publishing LLC*. [http://dx.doi.org/10.1063/1.4828705]

I. INTRODUCTION

Fluid transport through nanoscale channels is set to play an important role in many nanotechnology applications.[1,2] The major hurdle in the development of nanofluidic devices is the large power required to drive the fluid through nanochannels. Various methods have been proposed in the recent literature to drive fluid through nanochannels.[3,4] Thermal transpiration is one such method. This method is highly energy efficient since it can drive the fluid based on the temperature gradient developed as a result of the heat generated at the various parts of the device itself.

Thermal transpiration occurs when fluid molecules start moving from the cold end towards the hot end of a channel under the influence of longitudinal temperature gradient alone. This phenomenon was first observed in 1873 by an eminent Victorian experimenter Sir William Crookes. Later in 1879, Osborne Reynolds observed that a difference of temperature on the two sides of the porous plate might cause gas to pass through the plate, without any initial difference of pressure, or any difference in chemical constitution. His experiments showed that, with hydrogen gas on both sides of the porous plate, a difference of 160°F on the two sides of the plate produced a permanent pressure difference of an inch of mercury, the higher pressure being on the hotter side. He proposed to call the motion of gas caused by a difference of temperature as Thermal Transpiration.[5] Maxwell[6] did a detailed mathematical analysis of the same and proposed the following relationship:

$$U_{th} = a \bigtriangledown T, \tag{1}$$

where U_{th} is the maximum velocity in the channel, $\bigtriangledown T$ is the rate of variation of the fluid temperature along the axis of the channel, and a is constant.

The above concept can be further explained by considering two reservoirs filled with the same gas having the same pressure ($P_1 = P_2$) but at different temperatures ($T_1 < T_2$).[7] These two reservoirs are connected by a rigid channel, whose hydraulic diameter (h) is comparable to the mean free path (λ) of the fluid. If m is the mass of the gas molecules, n is the number density and $\bar{c}$ the average molecular speed, then the mass flux at the cold and hot ends of the channel are given by $m_1 n_1 \bar{c_1}$ and $m_2 n_2 \bar{c_2}$, respectively. We assume that the density of the fluid is proportional to the number density ($\rho \propto n$) and the temperature of the fluid is proportional to the square of the average molecular speed ($T \propto \bar{c}^2$). Under such free molecular flow conditions,

$$\frac{m_1 n_1 \bar{c_1}}{m_2 n_2 \bar{c_2}} \approx \frac{\rho_1}{\rho_2}\sqrt{\frac{T_1}{T_2}}. \tag{2}$$

If we use the equation of state ($P = \rho RT$) and assume the condition that both the reservoirs are at same pressure ($P_1 = P_2$), the above equation reduces to

$$\frac{m_1 n_1 \bar{c_1}}{m_2 n_2 \bar{c_2}} = \sqrt{\frac{T_2}{T_1}}. \tag{3}$$

Since $T_1 < T_2$, this ratio is greater than one. The above analysis indicates a flow creeping from the cold to the hot end of the channel. Inside the channel, the interaction of fluid molecules with the wall atoms is crucial and it has considerable influence on the observed phenomenon. In large channels, thermal transpiration can be explained as an equilibrium

a)Electronic mail: sarith@nitc.ac.in

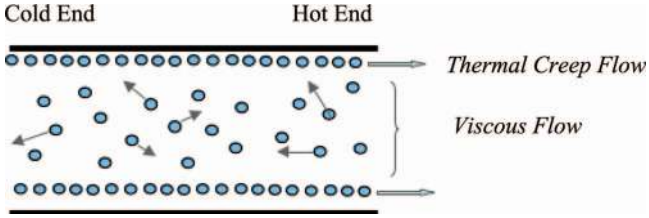

FIG. 1. A schematic diagram to explain thermal transpiration in large channels.

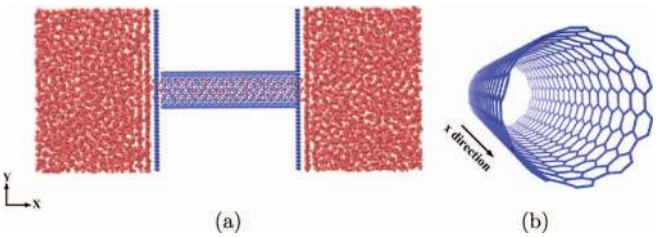

FIG. 2. A snapshot of the simulation box used in the present study. (a) Two reservoirs are connected using CNT. (b) Perspective view of the CNT.

state attained by two opposing flow fields, thermal creep flow that occurs from the cold to the hot end close to the channel walls and viscous flow (back flow) in the reverse direction at the central region of the channel due to the pressure difference. Figure 1 shows a schematic diagram of the flow field illustrating thermal transpiration in large channels.

In 1910, Knudsen first proposed the feasibility of a gas pump based on the phenomenon of thermal transpiration.[8] Such a pump would have the inherent advantage that they have no moving parts and are attractive for applications ranging from gas analysers to electronic cooling systems. For such a pump to operate near atmospheric pressure, these channels must have hydraulic diameter on the order of 100 nm or less. With recent advances in micromachining technology, it has been possible to fabricate flow channels with characteristic dimensions on the order of 100 nm. Atmospheric pressure operation of Knudsen pump was first demonstrated by Vargo and Muntz[9] and their device could generate a maximum pressure difference of 11.5 Torr (1.5 kPa) using helium. This was followed by the first fully micromachined Knudsen pump by McNamara and Gianchandani.[10]

Due to the important role of molecular level mechanisms, an atomistic simulation method like Molecular Dynamics (MD) is more suitable to study the temperature induced fluid transport through nanochannels. Han[11] has carried out MD simulations to study the thermophoresis in liquids, which is defined as the migration of a colloidal particle or large molecule in a solution in response to a macroscopic temperature gradient. MD computations have also been performed to study the thermophoretic motion of a water cluster inside a single walled carbon nanotube (CNT).[12,13] Recent literature reports various attempts made by researchers to study thermal transpiration using MD simulations. Atomistic simulations have been performed earlier to study the feasibility of a device that drives fluid in nanoscale channels using a temperature gradient.[14] They have observed that as the size of the system reduces various factors like structuring of the fluid atoms, increased viscosity, thermal contact resistance, etc. begin to influence the fluid flow. MD studies on the mechanism of fluid transport driven by a temperature gradient in nanochannels have shown that the fluid−wall interaction plays a critical role in determining the flow direction.[15] They have reported that for channels of very low surface energy fluid moves from high to low temperature, while for channels with high surface energy the fluid is pumped from low to high temperature. Computational studies have shown that a fluid can be continuously circulated by a symmetric temperature gradient in nanochannels of heterogeneous surface energies.[16,17] In all these cases, a temperature gradient is imposed on the channel walls and its effect on the fluid transport is analysed.

Atomistically smooth, well characterised open ended carbon nanotubes have been shown to offer unique possibilities as fluid conduits in many biological applications like drug storage and delivery.[18] Another allotrope of carbon, graphene, has also attracted the interest of researchers due to its unique properties like high specific surface area and good chemical stability which makes it an exciting material with immense application in nanoelectronics.[19] In the present work, MD simulations are carried out to investigate the occurrence of thermal transpiration of liquid argon through single walled CNT and graphene nanochannels. In order to develop a temperature gradient, two liquid reservoirs are created at the ends of the channel and are maintained at different temperatures.

II. SIMULATION DETAILS

Two different systems are considered where liquid argon is allowed to flow between the two reservoirs maintained at different temperatures. In the first system, the two reservoirs are connected by a CNT while in the second system the two reservoirs are connected by a graphene channel. Two graphene sheets are arranged parallel to each other for obtaining a graphene channel. Nonequilibrium molecular dynamics (NEMD) simulations were carried out using LAMMPS package[20] and the visualisations were rendered using VMD.[21]

A snapshot of the simulation box of the first system is shown in Fig. 2(a). The system consists of two reservoirs connected by a CNT. Both the reservoirs are of the same size (60 Å × 60 Å × 45 Å) and the length of the CNT is 47.95 Å. The reservoirs are bounded by graphene walls as shown in Fig. 2(a). The details of the CNTs used in the present study are given in Table I.

A snapshot of the simulation box of the second system is shown in Figure 3(a). The two reservoirs in this case are connected by a graphene channel. The dimensions of both the reservoirs are the same as that in the previous

TABLE I. Details of different CNTs used in the simulation.

Designation	Diameter in Å
(10,10)	13.56
(12,12)	16.27
(14,14)	18.98
(16,16)	21.69

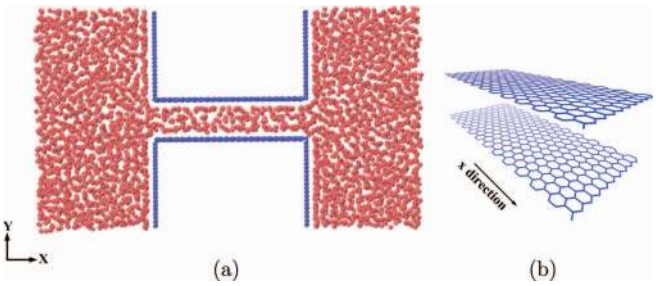

FIG. 3. A snapshot of the simulation box used in the present study. (a) Two reservoirs are connected using a graphene channel. (b) Perspective view of the graphene channel.

case. Length of the graphene channel is approximately 48 Å, which is also same as that of the CNTs. The width of the graphene nanochannel is taken as 24 Å. Four different channel heights are considered (13.56 Å, 16.27 Å, 18.98 Å, 21.69 Å). The interatomic interactions are modeled using the pairwise Lennard Jones (LJ) potential:

$$U_{LJ} = 4\varepsilon\left[\left(\frac{\sigma}{r}\right)^{12} - \left(\frac{\sigma}{r}\right)^{6}\right], \tag{4}$$

where r is the distance between a pair of interacting molecules and ε and σ are parameters describing the binding energy and bonding distance, respectively. The interaction parameters, $\varepsilon_{Ar-Ar} = 0.0098$ eV and $\sigma_{Ar} = 3.47$ Å were used for liquid argon.[15] For C-C interaction in the CNT, $\varepsilon_{C-C} = 0.0037$ eV and $\sigma_C = 3.4$ Å were used as LJ parameters.[22] $\varepsilon_{C-C} = 0.024$ eV and $\sigma_C = 3.34$ Å were used as LJ parameters for C-C interactions in graphene.[23–25] The Lorentz-Berthlot mixing rule was employed to calculate the LJ parameters for the interaction between the atoms of different types.[26]

The periodic boundary conditions were applied in all directions. The equations of motion were integrated using the velocity Verlet algorithm and a time step of 1 fs was used.[27] The number density ($\frac{N\sigma^3}{\Omega}$) of the fluid atoms in the reservoir was maintained around 0.8 and the channel walls were made rigid. Initially, the fluid atoms are prevented from entering into the channel by keeping a rigid graphene wall at both the ends of the channel. NVT ensemble was applied to the argon atoms kept in the two reservoirs. Langevin thermostat was applied to the argon atoms to maintain the temperature at 300 K. Simulations were performed for 50 ps. Then, the graphene walls at the ends of the CNT were removed and fluid atoms were allowed to enter and fill the CNT. During this process, NVT ensemble were applied to fluid atoms and the system was allowed to equilibrate by running the simulations for another 2 ns.

The properties of fluid atoms in nanoconfinements and its variation with channel size and temperature play a critical role in transport process. Two such properties, namely, diffusivity and viscosity are considered in the present study. The diffusion of gas molecules in nanochannels and its dependence on the channel size have been investigated earlier.[28] Since it is more appropriate to calculate the diffusivity at equilibrium conditions, separate simulations were carried out for calculating the same. After allowing the system to equilibrate, the fluid temperature is varied from 300 K to 450 K. The diffusion coefficient, D is calculated using the Einstein relation[29]

$$D = \frac{1}{2d}\lim_{t\to\infty}\frac{\langle|r(t) - r(0)|^2\rangle}{t}, \tag{5}$$

where r is the atom positions and d is the degree of dimensions. The flow of liquids through single walled CNT is considered as a 1D case. Taking $d = 1$ in the expression for diffusivity, the Eq. (5) reduces to

$$D = \frac{1}{2}\lim_{t\to\infty}\frac{\langle|r(t) - r(0)|^2\rangle}{t}. \tag{6}$$

Earlier studies have reported that confinements of fluids inside the CNTs reduce the viscosity of the fluid and it is found to vary nonlinearly with respect to the CNT diameter.[30] In the present study, we have used Eyring theory for calculating the viscosity of the confined fluid. Eyring theory employs the statistical mechanical theory of absolute reaction rates to analyse the transport mechanisms in fluids.[31] According to this theory, viscous flow is considered as a chemical reaction in which the elementary process is the activated jumping of a single molecule from one equilibrium position (minimum energy) to another. Hence for the flow to occur the molecules should possess the necessary energy to overcome this potential barrier. Activation energy, E_a is defined as the potential required by an individual molecule to overcome the potential barrier created by its neighbors and squeeze past them into the next equilibrium position. Following the method described in a previous study on viscosity of confined fluids, the following relations for the coefficient of viscosity can be obtained:[30]

$$\mu = \frac{Nh}{V}exp\left(\frac{E_a}{RT}\right), \tag{7}$$

where μ is the shear viscosity of the fluid, N is the Avogadros number, V is the molar volume, h is the Planck's constant, E_a is the activation energy, R is the Universal gas constant, and T is the temperature.

In the second step, in order to study the thermal transpiration phenomenon through the CNTs, temperature of one of the reservoirs is kept maintained at 300 K and the temperature of the other reservoir is varied from 370 K to 450 K. The simulations are performed for 2 ns to attain a steady flow rate and again run for a period of 1 ns to calculate the average fluid flow rate through the channel. Similar procedure is also followed for studying the thermal transpiration phenomenon through the graphene nanochannels.

III. RESULTS AND DISCUSSION

Simulations are carried out in two different steps. In the first step, the temperature of the fluid is varied from 300 K to 450 K. After allowing the system to reach equilibrium, the density distribution and the different viscoelastic properties inside the CNTs are evaluated. The variation of these properties with the CNT diameter and the fluid temperature are also analysed.

Figure 4 shows the density distribution inside a (10,10) CNT for temperatures 300 K and 450 K. From the figure, it

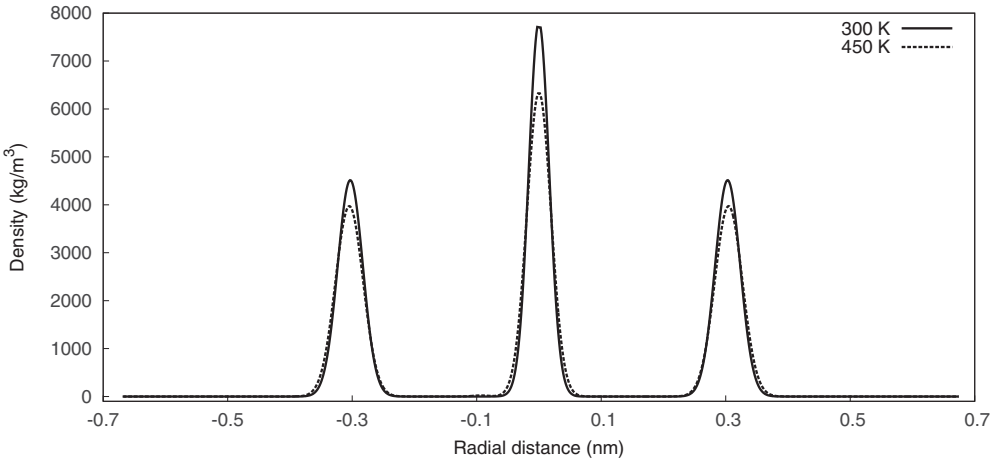

FIG. 4. Radial density distribution of confined fluid inside a (10,10) CNT at two different temperatures 300 K and 450 K.

is evident that in the case of smaller diameter nanotubes like (10,10) CNT, the confined fluid atoms are distributed in well-defined layers. The reason for the formation of such structures inside the CNTs is well attributed to the space confinement inside the nanotube and the fluid-wall interaction. From Fig. 4, it can be seen that as the temperature increases the density distribution gets broadened and the intensity of the peak reduces. This indicates that the layer formation is more prominent at lower temperatures. We have also analysed the variation in the density distribution with the diameter of the CNTs. Figure 5 shows the density distribution inside the (10,10) and (16,16) CNTs when the fluid temperature is 450 K. From Fig. 5, it can be seen that as the diameter of the CNT increases, the layered structure of the confined fluid molecules starts disappearing giving way to disordered bulk fluid arrangement.

The variation of viscoelastic properties of fluid atoms with respect to channel size and temperature plays a critical role in determining the density variation and fluid transport through narrow confinements. According to kinetic theory of liquids, properties like diffusivity and viscosity are found to influence the mobility of fluid atoms inside nanochannels.[32] In the present study, these two properties are evaluated to gain more insight into the molecular level mechanism of thermal transpiration.

Figure 6 shows the variation of self-diffusivity of argon atoms inside the CNTs with nanotube diameter for various temperatures. From the figure, it is clear that there is an increase in the diffusivity with the increase in the diameter and temperature. Figure 7 shows the variation of viscosity inside the CNTs with the nanotube diameter for various temperatures calculated using Eyring theory. The results indicate that there is an increase in the viscosity with the CNT diameter. Further with the increase in temperature, the viscosity was found to decrease. We have also used Green-Kubo formulation for calculating viscosity for a few cases. The values for viscosity obtained using Green-kubo formulation were not exactly same as that obtained using Eyring method. Nevertheless, they are of the same order of magnitude and showed similar variations.

In the second stage, we discuss the results of temperature driven fluid flow through nanoscale channels. In order to develop a temperature gradient inside the nanotube, temperature of one of the reservoirs is maintained at 300 K while the other is varied from 370 K to 450 K. Each data point corresponds

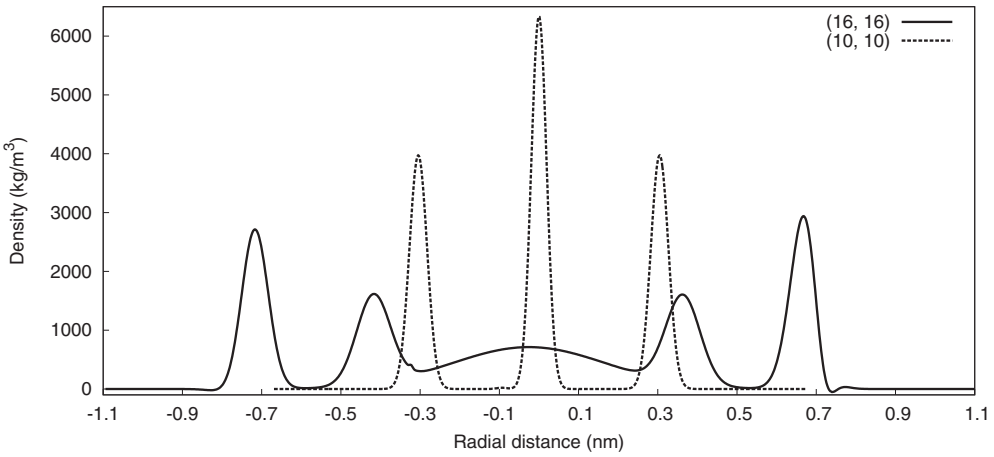

FIG. 5. Radial density distribution of confined fluid in (10,10) and (16,16) CNTs at 450 K.

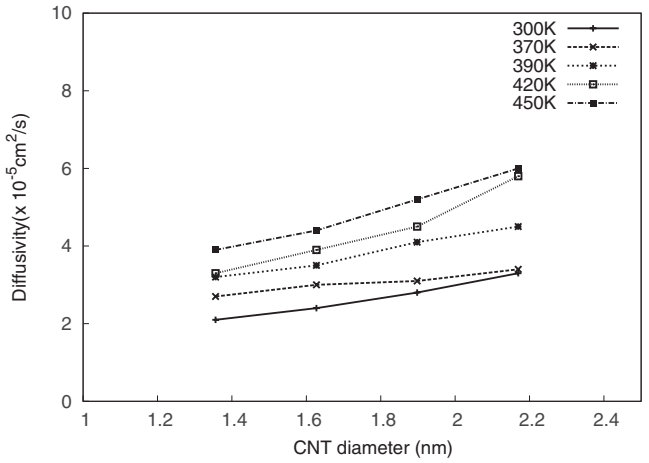

FIG. 6. The variation of self diffusivity of argon inside the CNTs with diameter.

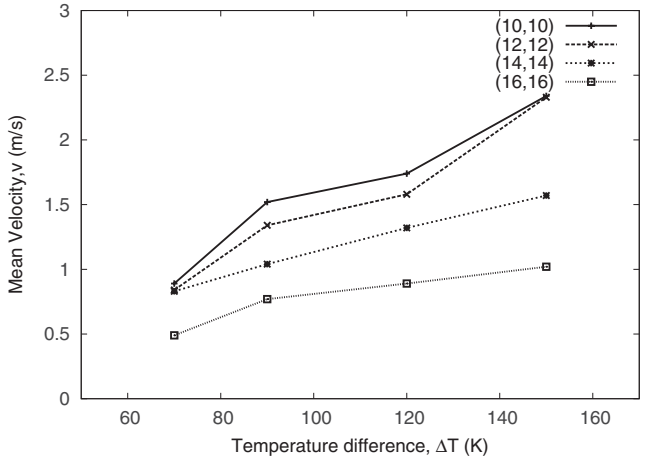

FIG. 8. The variation of mean velocity of the confined fluid inside the CNTs with temperature difference.

to an average value taken from five independent simulations with different initial conditions. In the present study, a positive value for mean velocity indicates that the flow occurs from the cold end to the hot end.

Figure 8 shows the variation of the mean velocity of the fluid atoms inside the nanotubes with temperature difference, ΔT for four different CNTs. It is observed that the mean velocity of the confined fluid increases with the increase in the temperature of the hot reservoir and decreases with an increase in the CNT diameter.

To examine the existence of temperature gradient inside the nanotube, the nanotube is divided into four bins along the length of the CNT and the variation in temperature is obtained. Figure 9 shows the variation of the fluid temperature along the flow direction inside the CNTs with the temperatures maintained at 300 K and 450 K for cold and hot reservoirs, respectively. The figure indicates a linear variation of temperature from the cold reservoir (300 K) to the hot reservoir (450 K), which asserts that there is a temperature gradient established among the fluid molecules inside the nanotube. It can also be seen that there is no significant variation in the temperature distribution among the different CNTs.

To further examine the temperature distribution inside the nanotube, the velocity distributions in the different bins are plotted. Figure 10 shows the velocity distribution inside a (10,10) CNT with the temperature of the two reservoirs maintained at 300 K and 450 K. The velocity distribution shows that there is a shift in the peak towards the larger velocity and the curve gets broadened as we move from the cold end to the hot end. This points towards the existence of a well defined temperature gradient inside the CNT which acts as a driving force for the fluid.

On the application of a temperature gradient, a variation of fluid density is observed in both the reservoirs and inside the CNT. The variation of normalised number density along the length of the CNT shows a gradual decrease in the flow direction (Fig. 11). The calculated number density has been normalised with the total number of fluid atoms present inside the corresponding nanotubes. At higher temperatures, the fluid molecules possess strong thermal vibrations. Due to the increased thermal motion, each fluid molecule tends to occupy a larger space. In physical terms, this manifests as a decrease in the number density at elevated temperatures. Further, due to the fluid-wall interaction, the fluid atoms form

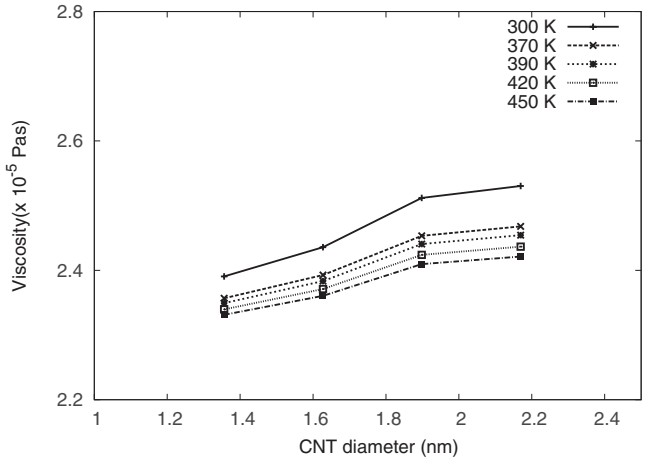

FIG. 7. The variation of viscosity of the confined fluid inside the CNTs with diameter.

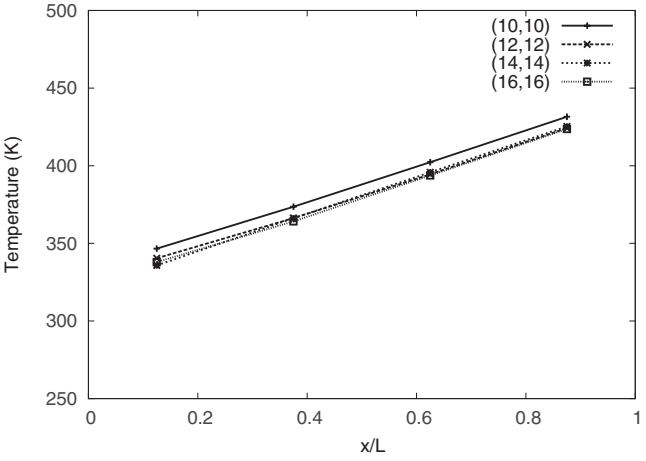

FIG. 9. The variation of the temperature of the confined fluid along the length of the CNTs.

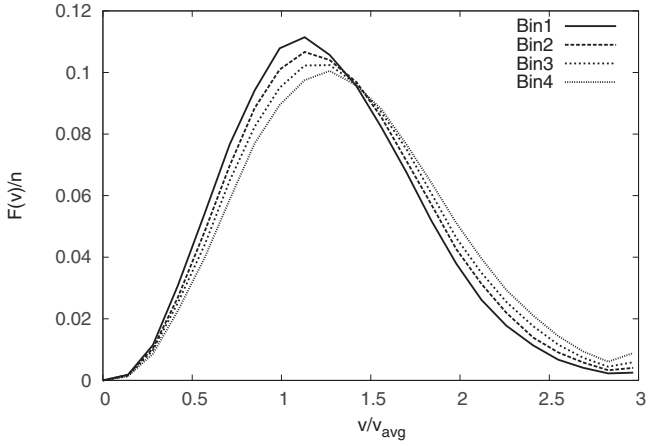

FIG. 10. Velocity distribution showing the mean number of molecules per unit volume having the speed v and v+dv inside a (10,10) CNT for a temperature difference of 150 K.

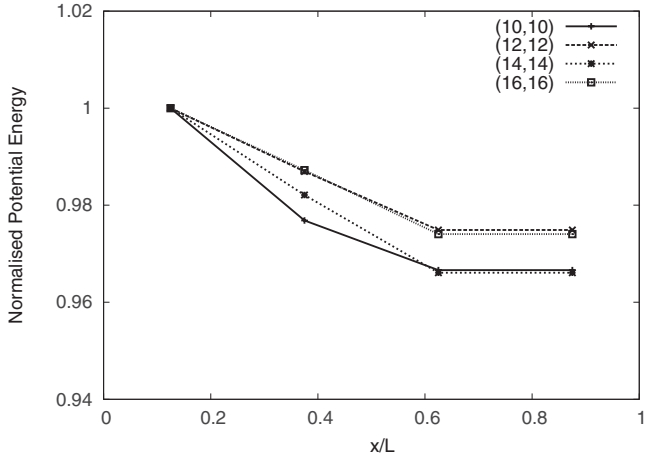

FIG. 12. The variation of normalised potential energy of the confined fluid along the length of the CNTs for a temperature difference of 150 K.

layers inside the CNTs and the graphene channels. From the variation of density distribution with temperature (Fig. 4), it is observed that the layering phenomenon is more prominent at low temperatures. Hence, on the application of a temperature gradient, a density variation is developed with in each fluid layer. Due to the above reasons, a density variation is established inside the nanochannels. The movement of molecules from the low temperature end to the high temperature end can be attributed to the combined effect of layer formation and density variation inside the CNTs. Thus, the density variation resulting from the temperature gradient is seen to be the major reason for the thermal transpiration in nanochannels.

Further, Fig. 12 shows the variation of normalised potential energy of argon atoms inside the CNT. The average potential energy is calculated and normalised using the maximum potential energy value in each case. The result indicates that, due to the temperature gradient, a potential energy gradient is developed along the length of the CNT. The density variation and the potential energy gradient developed inside the nanochannel produce a force on the fluid molecules, pushing them towards the high temperature reservoir.

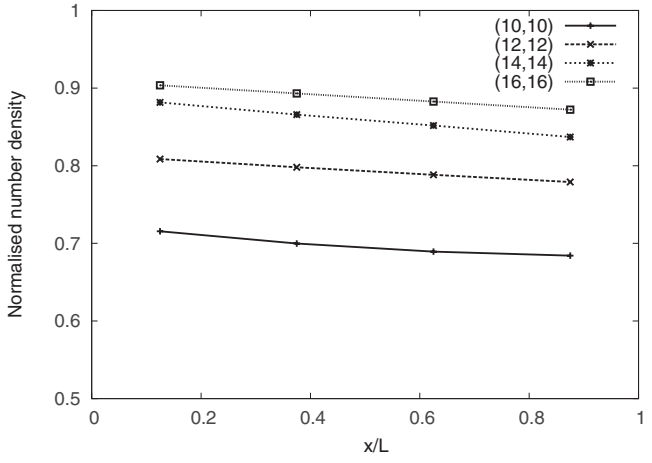

FIG. 11. The variation of normalised number density of the confined fluid along the length of the CNTs for a temperature difference of 150 K.

Results obtained from the equilibrium studies that we had presented earlier are further analysed to gain more insight into the underlying molecular level mechanism of thermal transpiration. From Fig. 5, it is clear that inside a (10,10) CNT, fluid molecules are arranged in distinct layers. As the diameter of the CNT increases, the molecular layers formed are present only near the walls of the tube and a viscous flow region develops at the center. This is evident from the density distribution inside a (16,16) CNT (Fig. 5). Since the layering of fluid atoms inside nanotubes is favorable for thermal creep, the thermal transpiration dominates in small diameter CNTs. Figure 6 shows that there is an increase in the diffusivity with an increase in the diameter. The increase in the diffusivity will enhance the mobility (average velocity acquired by them with respect to the surrounding particles) of the fluid atoms allowing them to move in a disordered manner.[32] This reduces the layering phenomenon and thus hinders the unidirectional motion of the fluid atoms. Together with the influence of the wall, it is this increase in the diffusivity that prevents the layering phenomenon in larger diameter channels. This in turn promotes counter flow thus reducing the mean velocity in larger diameter CNTs. The variation of viscosity with the diameter and the temperature also influences the fluid transport through nanotubes. As is observed from Fig. 7, the viscosity decreases with the increase in the temperature. The fluidity (capability of yielding to shearing stress) of the liquid, which is inversely proportional to the coefficient of viscosity, increases with the temperature.[32] It is obvious that, with the increase in the temperature gradient, the mean temperature of fluid atoms inside the CNT increases. Thus resistance to the flow of fluid atoms inside the CNTs is less at higher temperatures and hence an increase in the flow rate is observed at higher temperature gradients. Again the viscosity is found to increase with the increase in the CNT diameter. Thus in the case of the CNTs, smaller diameters and higher temperature gradients are more favorable for the occurrence of thermal transpiration.

In order to understand the flow pattern inside the nanotube, we analyse the velocity distribution along the cross section of the (10,10) and (16,16) CNTs for a temperature difference of 150 K. The velocity profile is shown in Fig. 13.

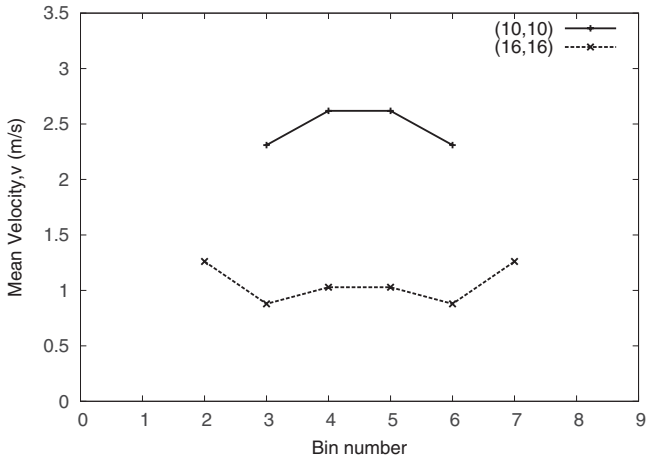

FIG. 13. Velocity profile of the confined fluid along the cross section of (10, 10) and (16, 16) CNTs for a temperature difference of 150 K.

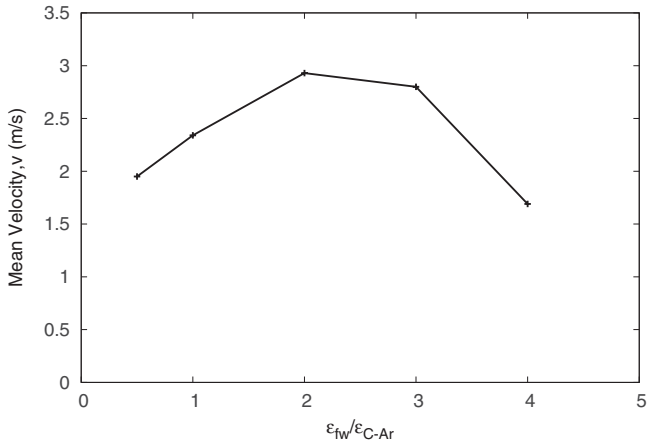

FIG. 14. The variation of mean velocity of confined fluid in (10, 10) CNT with fluid-wall binding energy.

Inside a (10,10) CNT, the fluid atoms are arranged in a concentric ring and a single file at the center. In such nanotubes, viscous flow region is absent and thermal creep dominates. Therefore, we obtain a flat velocity profile indicative of plug type flow inside such nanotubes. As the diameter of the CNT increases, a prominent viscous flow region is developed in the central region. This viscous region promotes the counter flow at the center. Hence, the fluid atoms inside a (16,16) CNT possess a larger velocity near the wall and a lower velocity at the center.

It is a well established fact that the liquid adjacent to a solid need not be stationary and may be subjected to slip. For nanoscale channels, slip velocity becomes significant. The velocity profile inside the CNTs showed considerable molecular slip at the boundaries. The velocity profile of the fluid in the channel is extrapolated at the interfaces and the slip length(l_s) is determined using the Navier boundary conditions[33]

$$l_s = \frac{u_{wall}}{(\frac{\partial u}{\partial z})_{wall}}, \tag{8}$$

where u_{wall} is the linear velocity of the fluid near the wall and $(\frac{\partial u}{\partial z})_{wall}$ is the velocity gradient at the wall obtained from the velocity profile. Calculated values of slip lengths are normalised using the maximum slip length and are shown in Table II. It can be seen that the slip length decreases with the increase in the CNT diameter. Lower slip length indicates a reduction in the fluid slip near the wall. However, for (16,16) CNT, the thermal creep flow was found to occur only near the wall and the viscous flow dominated in the central region. This result in a larger velocity near the wall and hence the slip length could not be calculated from the velocity profile.

TABLE II. Normalised slip length for confined argon in CNTs.

CNTs	Slip length (normalised)
(10,10)	1
(12,12)	0.86
(14,14)	0.76

Although the surface effects are not dominant in the present system (due to the weak fluid-wall interaction), it does have a considerable influence on the fluid molecules confined in smaller channels. We have tried to investigate the effect of the surface energy on the fluid molecules by varying the fluid-wall interaction strength, ε_{fw}. Figure 14 shows the dependence of the mean velocity of the fluid on the fluid-wall interaction strength, ε_{fw} for the (10, 10) CNT, with the high temperature reservoir maintained at 450 K. Initially, as ε_{fw} increases, the wall effect becomes important leading to density fluctuations in the fluid which creates a larger pressure drop. Thus, an increase in the mean velocity is observed with the increase in ε_{fw}. As ε_{fw} is further increased, the adsorption of the fluid molecules takes place. This will reduce the effective channel size resulting in a decrease in the fluid velocity. Similar observations have been already reported in the literature.[15]

The variation of mean velocity of fluid inside the (10, 10) CNT with fluid-fluid interaction strength, ε_{ff}, is shown in Fig. 15. The temperatures of the cold and hot reservoirs are maintained at 300 K and 450 K, respectively. A significant reduction in the mean velocity is observed as the fluid-fluid binding energy is increased. As ε_{ff} increases, the stronger fluid-fluid attraction imposes greater resistance to the fluid atoms entering into the nanotube, resulting in a decrease in the mean velocity.

In order to study the dependence of velocity on the geometry of the flow passage, we have replaced the CNT with two parallel graphene sheets. Simulations are repeated under the same conditions as that for the CNTs. We have chosen graphene for the channel wall as it is having lower interaction strength with Ar molecules and the ε values are close to those of CNT. Four different channel heights are considered whose values correspond to the diameters of the CNTs considered in the earlier simulations.

Figure 16 shows the variation of mean velocity of the fluid confined between the graphene sheets under the effect of a temperature gradient. Although the mean velocity of the fluid increases with the increase in the temperature gradient, the dependence of the mean velocity on the width of the graphene channel shows a different trend when compared to

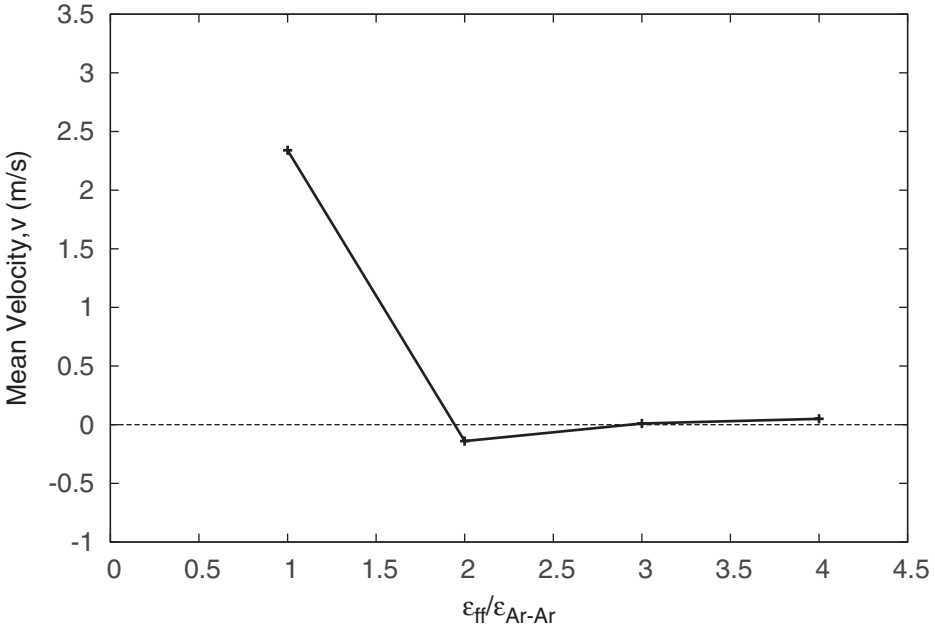

FIG. 15. The variation of mean velocity of fluid inside the (10, 10) CNT with fluid-fluid binding energy.

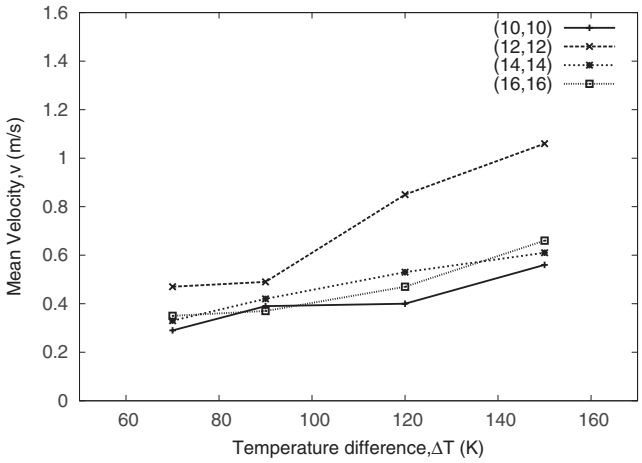

FIG. 16. The variation of mean velocity of the confined fluid with temperature difference inside the graphene nanochannels.

the CNTs. From Fig. 16, it is clear that, the physical condition of 16.27 Å wide channel is found to be more favorable for the thermal transpiration phenomenon. The reason behind the observed higher fluid velocity for the 16.27 Å wide graphene channel can be attributed to the layered arrangement of confined fluid atoms in the channel. The density profile shown in Fig. 17 indicates that larger number of liquid layers (four layers) are formed inside the 16.27 Å wide channel when compared to 13.56 Å wide channel (three layers). It is this increase in the number of fluid layers that leads to an increase in the mean velocity of fluid for the 16.27 Å wide channel. As the width of the channel is further increased (>16.27 Å), layered structure starts disappearing and the viscous flow starts dominating at the central region resulting in a decrease in the mean velocity. It is also observed that the mean velocity of the fluid inside the graphene channels is lower than that through the CNTs with similar dimensions. The decrease in the mean

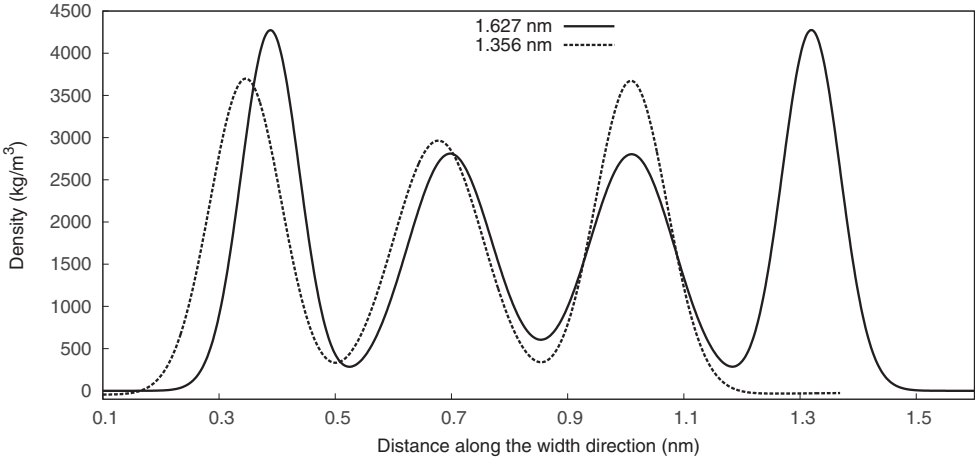

FIG. 17. The density distribution of confined fluid inside the graphene nanochannels at 450 K.

velocity could be attributed to the higher degree of fluid confinement that is observed inside the CNTs.

IV. CONCLUSION

In the present work, we have used MD simulations to study the fluid transport through the CNTs and the graphene nanochannels when subjected to a temperature gradient. In the case of the CNTs, thermal transpiration was observed and a consistent flow was developed from the cold end to the hot end of the channel. The mean velocity of the fluid atoms inside the CNT was found to increase with the increase in the temperature gradient and decrease with the increase in the nanotube diameter. Fluid-wall interaction strength (ε_{fw}), self-diffusion coefficient (D), and viscosity of the confined fluid (μ) were found to influence the flow rate inside the CNTs. Simulations carried out using graphene channels with similar conditions also showed the occurrence of thermal transpiration. However, the mean fluid velocity that developed inside the graphene channels was found to be lower than that observed in the CNTs with similar dimensions.

[1]H. A. Stone, A. D. Stroock, and A. Ajdari, Annu. Rev. Fluid Mech. **36**, 381 (2004).
[2]S. Ghosh, A. K. Sood, and N. Kumar, Science **299**, 1042 (2003).
[3]S. Pennathur and J. G. Santiago, Anal. Chem. **77**, 6772 (2005).
[4]M. Rauscher, S. Dietrich, and J. Koplik, Phys. Rev. Lett. **98**, 224504 (2007).
[5]O. Reynolds, Philos. Trans. R. Soc. London **170**, 727 (1879).
[6]J. C. Maxwell, Philos. Trans. R. Soc. London **170**, 231 (1879).
[7]G. Karniadakis, A. Beskok, and N. Aluru, *Microflows and Nanoflows: Fundamentals and Simulation* (Springer, New York, 2005).
[8]M. Knudsen, Ann. Phys. **31**, 205 (1910).
[9]S. E. Vargo and E. P. Muntz, AIP Conf. Proc. **585**, 502 (2001).
[10]S. McNamara and Y. B. Gianchandani, J. Microelectromech. Syst. **14**, 741 (2005).
[11]M. Han, J. Colloid Interface Sci. **284**, 339 (2005).
[12]J. Shiomi and S. Maruyama, Nanotechnology **20**, 055708 (2009).
[13]H. A. Zambrano, J. H. Walther, P. Koumoutsakos, and I. F. Sbalzarini, Nano Lett. **9**, 66 (2009).
[14]M. Han, J. Mech. Sci. Technol. **22**, 157 (2008).
[15]C. Liu, Y. Lv, and Z. Li, J. Chem. Phys. **136**, 114506 (2012).
[16]C. Liu and Z. G. Li, AIP Conf. Proc. **1376**, 610 (2011).
[17]C. Liu and Z. Li, Phys. Rev. Lett. **105**, 174501 (2010).
[18]A. Bianco, K. Kostarelos, and M. Prato, Curr. Opin. Chem. Biol. **9**, 674 (2005).
[19]H.-J. Choi, S.-M. Jung, J.-M. Seo, D. W. Chang, L. Dai, and J.-B. Baek, Nano Energy **1**, 534 (2012).
[20]S. Plimpton, J. Comput. Phys. **117**, 1 (1995).
[21]W. Humphrey, A. Dalke, and K. Schulten, J. Mol. Graphics **14**, 33 (1996).
[22]G. Hummer, J. C. Rasaiah, and J. P. Noworyta, Nature (London) **414**, 188 (2001).
[23]K. Saitoh and H. Hayakawa, Phys. Rev. B **81**, 115447 (2010).
[24]D. D. Do and H. D. Do, Adsorpt. Sci. Technol. **21**, 389 (2003).
[25]A. Wongkoblap, D. D. Do, and D. Nicholson, Phys. Chem. Chem. Phys. **10**, 1106 (2008).
[26]P. M. Agrawal, B. M. Rice, and D. L. Thompson, Surf. Sci. **515**, 21 (2002).
[27]M. P. Allen and D. J. Tildesley, *Computer Simulation of Liquids* (Oxford University Press, Oxford, 1987).
[28]Z. Li and L. Hong, J. Chem. Phys. **127**, 074706 (2007).
[29]Y. Liu and Q. Wang, Phys. Rev. B **72**, 085420 (2005).
[30]J. S. Babu and S. P. Sathian, J. Chem. Phys. **134**, 194509 (2011).
[31]H. Eyring, J. Chem. Phys. **4**, 283 (1936).
[32]J. Frenkel, *Kinetic Theory of Liquids* (Dover Publications, New York, 1955).
[33]T. G. Myers, Microfluid. Nanofluid. **10**, 1141 (2011).